Electron beam assisted field evaporation of insulating nanowires/tubes

N. P. Blanchard, A. Niguès, M. Choueib, S. Perisanu, A. Ayari, P. Poncharal, S. T. Purcell, A. Siria, and P. Vincent

Citation: Appl. Phys. Lett. **106**, 193102 (2015); doi: 10.1063/1.4921166
View online: http://dx.doi.org/10.1063/1.4921166
View Table of Contents: http://aip.scitation.org/toc/apl/106/19
Published by the American Institute of Physics

Electron beam assisted field evaporation of insulating nanowires/tubes

N. P. Blanchard,[a] A. Niguès, M. Choueib, S. Perisanu, A. Ayari, P. Poncharal, S. T. Purcell, A. Siria, and P. Vincent
Institut Lumière Matière, UMR5306 Université Lyon 1-CNRS, Université de Lyon, 69622 Villeurbanne Cedex, France

(Received 9 January 2015; accepted 5 May 2015; published online 12 May 2015)

We demonstrate field evaporation of insulating materials, specifically BN nanotubes and undoped Si nanowires, assisted by a convergent electron beam. Electron irradiation leads to positive charging at the nano-object's apex and to an important increase of the local electric field thus inducing field evaporation. Experiments performed both in a transmission electron microscope and in a scanning electron microscope are presented. This technique permits the selective evaporation of individual nanowires in complex materials. Electron assisted field evaporation could be an interesting alternative or complementary to laser induced field desorption used in atom probe tomography of insulating materials. © *2015 AIP Publishing LLC*. [http://dx.doi.org/10.1063/1.4921166]

Atom probe tomography[1–3] (APT) is a powerful tool for studying metals and alloys, permitting 3D analytical mapping with atomic resolution. APT offers unique insights into both the chemical composition and atomic structure of matter. Initially, APT used High Voltage (HV) pulsed field evaporation (FE) of surface atoms from needle shaped specimens.[4] The applied HV pulse induces an electric field that is sufficient to field evaporate atoms from the tip surface which are then positioned and chemically identified by a time resolved position-sensitive detector.

However, in the case of materials with poor electrical conductivity, i.e., semiconductors or insulators, the HV pulses cannot be properly transmitted to the apex due to the high RC time that acts as a low pass filter. Several studies on semiconductors by HV pulsing APT were initiated in the 1970s, essentially on silicon based materials. These studies reported the maximal value of the resistivity to be 10–100 Ω·cm (Refs. 5 and 6) for exploitable results. Melmed *et al.*[7] published measurements on higher resistivity samples (from 10^3 to 10^4 Ω·cm) by increasing the pulse duration to a few hundreds of ns; however, this distortion degrades the time resolution which in turn degrades the mass resolution.

Since 2006, the use of sub-nanosecond, picosecond, or even femtosecond lasers has seen the development of laser pulsed APT. It is now widely accepted that laser pulsed FE is thermally activated,[8] therefore circumnavigating the above mentioned problems associated with certain materials' poor electrical conductivity. Laser pulsed APT has been reported for Si,[9] Ge,[10] GaN,[11] and GaAs[12] with a growing interest of studying semiconductor nanowires (NWs) due to their potential use in future nano-electronic and nano-optoelectronic devices. However, making tips with individual NWs is still a tricky procedure that limits systematic studies. Developing alternative techniques that do not necessarily require a tip geometry could be advantageous for investigating highly resistive or insulating NWs by APT. We propose a method using a convergent electron beam whose implementation in APT could permit the study of insulating materials with unprecedented selectivity.

In this paper, we describe and analyze the electron beam assisted FE phenomenon of insulating materials. First, we describe experiments on BN nanotubes (NTs) and undoped Si NWs, both in a Transmission Electron Microscope (TEM), which allows a simultaneous control of the irradiation dose and the characterization of the desorption, and in a Scanning Electron Microscope (SEM). We go on to detail the electron-sample interactions that are at the origin of the FE. We propose that this electron beam assisted FE coupled with classical HV pulsed APT could permit the analysis of insulating materials. Modeling and estimations are made that confirm this approach. Finally, we conclude with a general discussion on the potential interest of this technique for APT.

TEM experiments were performed using an in-house built sample holder as presented previously[13–15] and in Fig. 1(g). The distance between the tip and the counter electrode is modifiable *in-situ*. The different samples were glued at the apex of etched tungsten tips and all the desorption experiments were performed at room temperature. Typically, for single BN NTs,[16] the NT-electrode distance is a few tens of μm with an applied DC voltage of a few hundred volts. With the BN tube at the standard focal plane of the objective lens, the electron beam is condensed on the BN tube's apex. The DC voltage for which electron beam evaporation begins varies from sample to sample and in some cases occurs even without an applied DC voltage. However, generally, voltages between 0.5 and 1.5 kV are required. If for a given voltage no evaporation is observed with a fully condensed e-beam, the DC voltage is increased, generally by 100 V steps, and the procedure is repeated until evaporation starts (Figure 1). The tube begins shortening until the extremity moves out of the irradiation zone or until reaching a defect, for example, a larger diameter. To continue the desorption, the electron beam is moved to follow the new apex position (see Figs. 1(a)–1(f)). We observed two mechanisms for BN tube FE.[15] In most cases, the evaporation starts with the outer walls being torn away analogous to a banana being peeled. When we continue FE, the inner part of the tube evaporates coming

[a]Electronic mail: nicholas.blanchard@univ-lyon1.fr

 © AIP Publishing LLC 2015

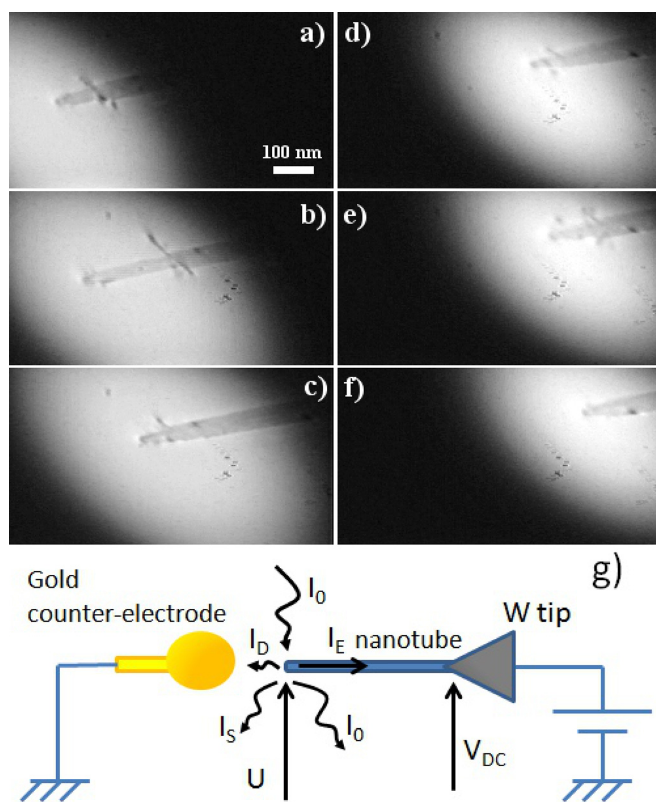

FIG. 1. Electron beam assisted evaporation of a BN nanotubes. The images were recorded on the TEM phosphor screen. All images are at the same scale so that the shortening of the tube can be followed. From (a) to (f): Evolution of the nanowire's extremity during evaporation. A movie is available in the supplementary material.[15] (g) Schematic representation of the *in-situ* field evaporation geometry and the possible ion/electron currents.

closer to the peeled outer BN sheets. Once the inner walls have reached the peeled outer sheets, the process repeats. The second mechanism sees the tube's extremity taking on a conical shape with the evaporation reducing the NT's length rather like a lit cigarette. For some samples, the evaporation mechanism evolves between the two scenarios. We believe that the first "peeling" mechanism is related to the defects present in the layered structure of the BN tubes. High resolution images of BN tubes often show defects and sometimes empty cavities located inside the NT walls.[17] These defects strongly reduce the Van der Waals' interactions between the different layers and when the extremity of the NT is evaporated the coulomb repulsion between layers becomes predominant, leading to the peeling of the external layers. While opening, these layers are rapidly evaporated due to their small dimensions and once the evaporation has ended we observe layers perpendicular to the tube axis. On the contrary, if no defects are present, the cohesion forces prevent coulomb explosion and the field evaporation reduces the extremity in a classical manner. For non-layered materials, such as silicon NWs, we only observed the classical FE with the formation of a smooth surface that recedes gradually.

The crucial role of the electron beam in this desorption mechanism is emphasized by experiments with nanowire/tube carpets, where individual nanopillars can be selectively evaporated one by one. Fig. 2(a) (upper) presents two close BN tubes. Initially, the electron beam was condensed at the end of the longest NT (Fig. 2(b)). Then, the beam was focused on the smaller neighboring NT (Fig. 2(c)) without further modifying the longer one. This clearly shows that the irradiation by the electron beam is the key parameter for this FE configuration (see film in supplementary material[15]) and proves the selectivity of our technique determined by the diameter of the electron beam which is orders of magnitude smaller than optical focusing. To further examine the potential of this electron beam induced evaporation on other materials, we carried out additional experiments on intrinsic Si NWs.[18] Fig. 2 (lower) presents the FE of a NW with a large defect at its apex. Such a geometry requires in the classical FE configuration a higher external voltage to achieve a high enough local electric field for evaporation and when the defect is removed, the smaller apex radius for the same external voltage can result in a very rapid shortening of the wire. However, by taking advantage of the electron beam assisted evaporation, a smooth tip apex can be achieved in a controllable manner.

The configuration for experiments realized in the SEM was identical to those in the TEM. A BN NT/W tip sample was connected to a positive HV source and another tip was positioned with piezo-motors close to the NT to serve as a

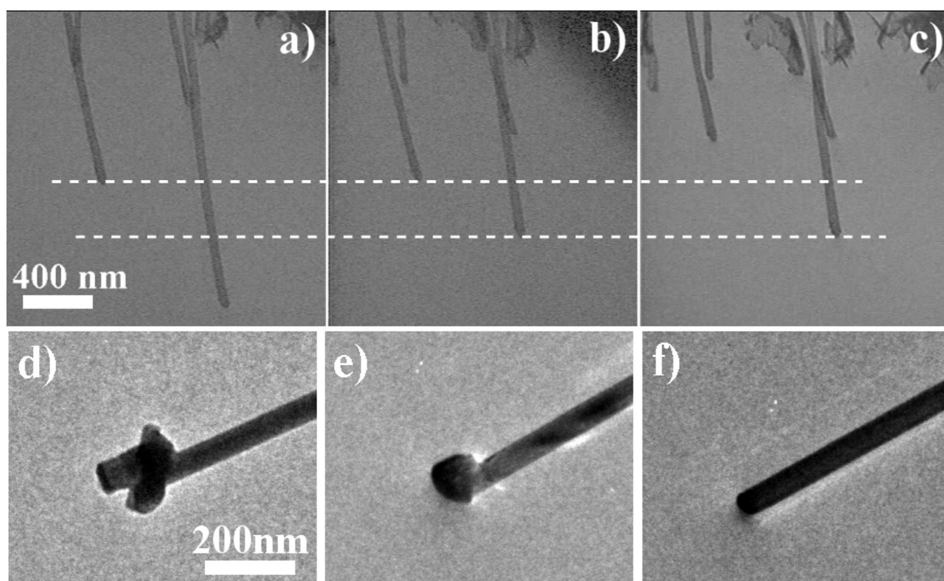

FIG. 2. TEM images obtained during the electron beam assisted field evaporation of BN NTs (upper) and an intrinsic Si nanowire (lower). (a) Initial configuration with two close BN NTs. (b) Image of the NTs after selectively evaporating the longer one by concentrating the beam at its extremity. (c) The same procedure applied to shorter tube without modifying the longer tube (see supplementary material for the corresponding movie[15]). (d) Image of an intrinsic Si nanowire with large defect at the apex prior to evaporation. (e) Image after field evaporation has begun. The defect has been reduced and presents a smoother surface. (f) Nanowire with a smooth hemispheric apex at the end of the experiment.

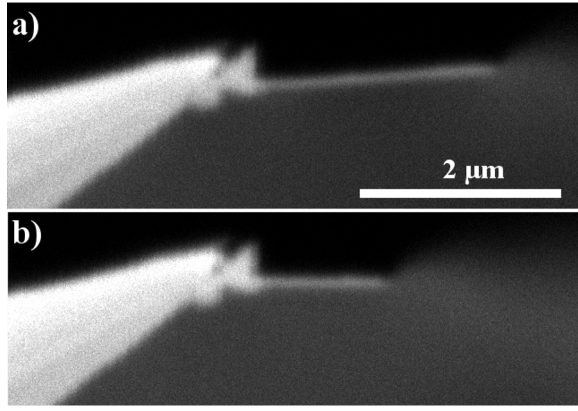

FIG. 3. Electron beam assisted field evaporation performed in a SEM. (a) BN NT mounted on a tungsten tip before field evaporation. The rather poor quality of the image is mainly due to the polarization of the tip to +800 V. (b) Image after evaporation showing a shortening >1 μm. The procedure used in SEM is described in more detail in the supplementary material.[15]

cathode. The support tip is first held at a positive voltage before imaging, to prevent the bending and sticking of the nanowire on the tungsten support tip during imaging,[19] and the image magnification was increased until the image of the NT covers a large part of the display screen (see Figure 3). The scanned area was reduced while keeping the nanowire's extremity at the center of the scanned zone. With the correct choice of e-beam current and accelerating voltage, we observed evaporation from the extremity of the wire. The experimental parameters for the desorption in Fig. 3 were a current of 5.1 nA and an acceleration voltage of 10 kV.[15]

Electron irradiation effects of thin insulating materials have been studied (e.g., Cazaux[20] and references therein) principally for foil structures. In general, the incident electrons are too energetic to be absorbed by a thin sample but they can initiate the ionization of atoms leading to the emission of secondary, Auger, and core electrons into the vacuum. These electron emission phenomena lead to insulating specimens acquiring a net positive charge. In metallic samples, this positive charge is compensated by a current of electrons conducted into the irradiation zone from the surroundings; however, for insulating materials, the poor electrical conductivity inhibits the neutralization of the radiation induced net positive charge. Net charge leads to a voltage increase, controlled by the capacitive environment, and can finally result in large electric fields which are further enhanced by the nanowires' tip geometry. The additional electric field at the apex of the wire can be high enough for FE. In this ultimate case, the ionic current leaving the wire prevents higher charging and therefore greater electric fields. This configuration is illustrated schematically in Fig. 1(g), which depicts the nanowire held at a positive voltage, V_{DC}, in front of a counter electrode. The potential at the nanowire's apex is U, with $U > V_{DC}$. I_0 is the electron beam arriving and leaving the nanowire (i.e., assuming no absorption); I_S is the current coming from secondary, Auger, and core electrons; I_E is the neutralization current through the nanowire; and I_D is the ionic current in the case of field evaporation. The important parameters to estimate are the maximum voltage (and field) at the apex and the associated time scale. This aspect is fundamentally related to the value of I_E, i.e., the insulating behavior of the nanowire, and the evolution of I_S (that is the contributions of secondary, Auger, and core electrons) versus $U - V_{DC}$. Typically, the different contributions to I_S are

(i) Secondary electron (SE) emission dominates this current. The SE yield is high and can reach more than 10 for certain insulating materials. However, it is mostly composed of electrons having a kinetic energy below 50 eV and thus it decreases markedly when the apex potential increases positively. Therefore, this emission is predominant for dynamic aspects (as for HV-pulsing mode) but cannot explain voltage increases above 50 V.

(ii) Auger electrons are generated in the wire, which depends on its atomic composition. For BN and Si, these Auger electrons can cause voltage increases up to 400–500 V.

(iii) the last contribution corresponds to the direct emission of core electrons into the vacuum. Though the yield is even lower, these electrons can have a higher energy.

In the following, we will focus on two aspects: (1) confirming that for highly insulating materials the electron charging results in a voltage and field magnitude compatible with FE and (2) show that this technique can be of interest for HV field evaporation of insulating materials.

For the first point, rough estimations of the order of magnitude are often made using the relation $F = V/\kappa r$ where F is the local electric field, V is the applied voltage, r is the tip radius, and κ is the field reduction factor generally around 5 for classical metallic tips and around 4 for long NWs. Here, the situation is rather more complicated, since the voltage is the result of the addition of the DC voltage applied to the tip plus the voltage increase in the wire due to electron charging (see supplementary material[15]). According to the superposition principle, we can write the field approximation as

$$F = \frac{V_1}{\kappa_1 r} + \frac{V_2}{\kappa_2 r}, \tag{1}$$

where V_1 is the DC voltage to the tip, κ_1 is the classical reduction factor, V_2 is the voltage increase along the wire, and κ_2 is a new reduction factor that does not take into account the shielding of the tip. By finite element simulations, we estimate that κ_2 should be around 2. Taking $V_1 = 1000$ V, $V_2 = 500$ V, and $r = 25$ nm for our sample and $\kappa_1 = 4$ and $\kappa_2 = 2$, this gives a field in the 2.0×10^{10} V·m^{-1} which is in the range required for FE.

The second point deals with the possibility to use this technique for insulating materials via the HV pulsing APT. The underlying idea is that the SEs produced by the primary electrons act as a short that strongly reduces the charging time compared to classical RC charging. Complete analysis of the problem can be found in the supplementary information;[15] however, for the limiting case, where all the charges come from the SEs, the charging time is given by

$$T_1 = \frac{CV}{\delta_m i_0}, \tag{2}$$

where C is the capacitance between the nanowire and the surrounding electrodes, V is the voltage pulse, δ_m is the SE yield, and i_0 is the primary current. Remarkably, this value is independent of the wire's resistance. Taking $C = 10^{-17}\ F$, $V = 200\,V$, $\delta_m = 5$, and $i_0 = 40\,nA$, one obtains $T_1 = 10\,ns$, which is compatible with the duration usually employed for HV pulsed APT. This time interval could be further reduced either by increasing the primary e-beam current or optimizing the e-beam landing energy to maximize the SE yield. Complementary discussion can be found in the supplementary material,[15] but this clearly establishes the interest of the technique for insulating materials that could until now only be studied by laser pulsed APT.

A direct comparison of our preliminary studies to laser pulsed APT is not yet possible; however, some advantages of electron beam assisted FE with a SEM can be postulated:

- Modern SEMs are much simplified and allow rapid NT/NW selection resulting in an unprecedented selectivity; an advantage for the analysis of more complex samples such as as-grown NW/NT on substrates.
- The integration of a SEM column would allow, in principle, the addition of detectors and analysis based on electron irradiation such as an Electron Backscatter Diffraction camera to probe the sample's structure. Moreover, different options could be used such as a sub-ns shutter for pulsed e-beam irradiation.
- Finally, the combination of a femtosecond laser and an electron column in an APT could lead to a versatile analysis system. One may imagine using the electron beam to selectively increase the electric field on a particular nano-object in a complex configuration with other close objects in combination with laser pulses to evaporate only this object and take advantage of optimized triggered detection.

From an instrumentation perspective, a SEM column should be integrated into an APT to confirm the potentialities of the technique for insulating materials. Further improvement will come about by acquiring a greater understanding of electron-sample interactions within insulating materials having a thin needle shape.

In conclusion, we have demonstrated electron beam assisted FE of highly insulating NTs and NWs. We have shown that this technique permits a high selectivity of the object to be evaporated. We presented a model based on the positive charging of the nano-object that allowed us to estimate a local electric field whose magnitude is compatible with field evaporation. Finally, we proposed that this technique could be interesting for HV pulsed APT. We are confident that this electron beam assisted FE can be applied to the development of APT for insulating materials which is an evolving and promising field.

We thank Mickael Bechelany for the BN nanotubes and Costel Cojocaru for the Si nanowires. This work was supported by the French National Research Agency (ANR) through its Nanoscience and Nanotechnology Program (Mikado, ANR-09-NANO-018-01BIS MIKADO) and the Cluster MACODEV of the Région Rhône-Alpes (cluster 3 SRESR 2010 (réf. 10 016913 01)). The authors acknowledge the Plateforme Nanofils et Nanotubes Lyonnaise of the University Lyon1.

[1] B. Gault, M. P. Moody, J. M. Cairney, and S. P. Ringer, *Atom Probe Microscopy* (Springer, New York, 2012).
[2] D. Blavette, B. Deconihout, A. Bostel, J. M. Sarrau, M. Bouet, and A. Menand, Rev. Sci. Instrum. **64**, 2911 (1993).
[3] T. F. Kelly and M. K. Miller, Rev. Sci. Instrum. **78**, 031101 (2007).
[4] E. W. Müller, J. A. Panitz, and S. B. McLane, Rev. Sci. Instrum. **39**, 83 (1968).
[5] A. J. Melmed, T. Sakurai, Y. Kuk, and E. I. Givargizov, Surf. Sci. **103**, L139 (1981).
[6] M. Gilbert, F. Vurpillot, A. Vella, H. Bernas, and B. Deconihout, Ultramicroscopy **107**, 767 (2007).
[7] A. J. Melmed, M. Martinka, S. M. Girvin, T. Sakurai, and Y. Kuk, Appl. Phys. Lett. **39**, 416 (1981).
[8] T. F. Kelly, A. Vella, J. H. Bunton, J. Houard, E. P. Silaeva, J. Bogdanowicz, and W. Vandervorst, Curr. Opin. Solid State Mater. Sci. **18**, 81 (2014).
[9] T. J. Prosa, R. Alvis, L. Tsakalakos, and V. S. Smentkowski, J. Microsc. **239**, 92 (2010).
[10] D. E. Perea, E. R. Hemesath, E. J. Schwalbach, J. L. Lensch-Falk, P. W. Voorhees, and L. J. Lauhon, Nat. Nanotechnol. **4**, 315 (2009).
[11] R. Agrawal, R. A. Bernal, D. Isheim, and H. D. Espinosa, J. Phys. Chem. C **115**, 17688 (2011).
[12] S. Du, T. Burgess, B. Gault, Q. Gao, P. Bao, L. Li, X. Cui, W. K. Yeoh, H. Liu, L. Yao, A. V. Ceguerra, H. H. Tan, C. Jagadish, S. Ringer, and R. Zheng, Ultramicroscopy **132**, 186 (2013).
[13] P. Poncharal, P. Vincent, J.-M. Benoit, S. Perisanu, A. Ayari, M. Choueib, and S. T. Purcell, Nanotechnology **21**, 215303 (2010).
[14] J. Shen, P. Vincent, N. P. Blanchard, J. Nicolle, M. Choueib, S. T. Purcell, and P. Poncharal, J. Vac. Sci. Technol. B **30**, 011801 (2012).
[15] See supplementary material at http://dx.doi.org/10.1063/1.4921166 for additional discussion and data.
[16] M. Bechelany, A. Brioude, S. Bernard, P. Stadelmann, D. Cornu, and P. Miele, CrystEngComm **13**, 6526 (2011).
[17] J. Garel, I. Leven, C. Zhi, K. S. Nagapriya, R. Popovitz-Biro, D. Golberg, Y. Bando, O. Hod, and E. Joselevich, Nano Lett. **12**, 6347 (2012).
[18] M. Choueib, R. Martel, C. Cojocaru, A. Ayari, P. Vincent, and S. T. Purcell, ACS Nano **6**, 7463 (2012).
[19] P. Vincent, S. Perisanu, A. Ayari, M. Choueib, V. Gouttenoire, M. Bechelany, A. Brioude, D. Cornu, and S. T. Purcell, Phys. Rev. B **76**, 085435 (2007).
[20] J. Cazaux, Ultramicroscopy **60**, 411 (1995).